Structural Characteristics of the Racing Car
in the Student Formula SAE Competition

by

Nanami YAMANOUCHI[*1], Koki ISHII[*1], Hiroyuki MORIYAMA[*2] and Hideaki KATO[*3]

Abstract

This paper describes structural characteristics of the racing car for the Student Formula SAE Competition of Japan and the monocoque structure of the main vehicle body. The structural characteristics are considered numerically by analysing the entire monocoque by FEM, in which the monocoque structure is subjected to external forces in the directions of compression, pitch, yaw and roll. The stress distribution and deformation were obtained from the analysis. With respect to the cross-section of the monocoque structure under deformation, the moving distance of the centroid and variation in the sectional secondary moment are examined as significant factors. As a result, the area where the stress becomes larger is distributed widely, thus verifying the monocoque characteristics by which the internal forces are dispersed throughout the whole structure. The moving distance of the centroid depends strongly on the load direction and increases greatly due to this correspondence with the load direction. Therefore, the structural rigidity can be evaluated by comparison of the moving distance. The ratio between the sectional secondary moments based on loaded and unloaded situations is used as a factor for evaluating structural rigidity, so the evaluation can accurately grasp the rigidity and also makes it possible to determine weak points of the monocoque structure.

Keywords: Student formula, Monocoque structure, Centroid of cross section, Sectional secondary moment

1. Introduction

The honeycomb structure, which is used in the fields of racing cars, high-speed rails and aerospace, attracts attention as a structural element with lightweight and high rigidity, and has been studied through theoretical, numerical and experimental approaches. Here, we take note of the racing car for Student Formula SAE Competition of Japan, whereas a space frame structure is adopted in a lot of student formula teams, having characteristics of inexpensive manufacturing costs and easiness of design, manufacturing and correction[1-3]. However, recently, a carbon monocoque structure tends to be adopted in domestic and foreign teams, enabling to attain light weight and high rigidity at the same time, so that some of them have gotten good results[4-7].

Since 2013, TFC (Tokai Formula Club) has adopted a carbone monocoque structure as the main vehicle body and has reconsidered the structural design to aim at lighter weight

and higher rigidity. However, the references to utilize for the above reconsideration are hardly found and the monocoque structure is designed by trial and error, so that the rational design method has not been established yet. In general, although theoretical and numerical analyses are employed in the design process of monocoque structure, the strength and rigidity are estimated based on the maximum stress and deformation in those solutions. To establish the rational design method, it is important not only to rely on published references but also to accurately evaluate own monocoque structures that were designed before.

This study takes note of the monocoque structure for Student Formula, which was designed by TFC and actually took part in that competition. The structural characteristics are investigated numerically by analysing the entire monocoque in FEM, from which the stress distribution and deformation are obtained as analysis results. In particular, with respect to the cross-section of the monocoque structure from the deformation, the moving distance of the centroid and variation in the sectional secondary moment are examined as significant factors for evaluating its structural rigidity.

*1 Undergraduate Student, Department of Prime Mover Engineering
*2 Professor, Department of Prime Mover Engineering
*3 Junior Associate Professor, Department of Prime Mover Engineering

2. Numerical Analysis Method

2.1 *Analytical model*

The paper takes about two kinds of racing cars that were produced by TFC, as shown in Fig. 1. They are denoted by Model A and B, which have respective specifications shown in Table 1. Although both models adopt a carbone monocoque structure as the main vehicle body in order to attempt their lightweight and high rigidity, the design and production of Model B is newer than those of Model A.

Figure 1 shows the analytical model to carry out actually the numerical analysis in ANSYS. The coordinates are set as X, Y and Z in this figure and the monocoque body is fixed at the square portions surrounded by red circles, which are in its rear part, in all directions of these axes. The external forces are applied to the square portions surrounded by yellow circles, which are in the front part of the monocoque body, along the respective axes.

2.2 *Multiscale analysis*

The above monocoque structure has been constructed of a honeycomb structure made by aluminum alloy and its surface plates made by CFRP. Although we employ FEM as a numerical method in such a honeycomb structure, the direct method with microscale model, which must mesh in the entire structure, not only brings a lot of the analysis time in FEM, but also can make FEM infeasible due to our computer
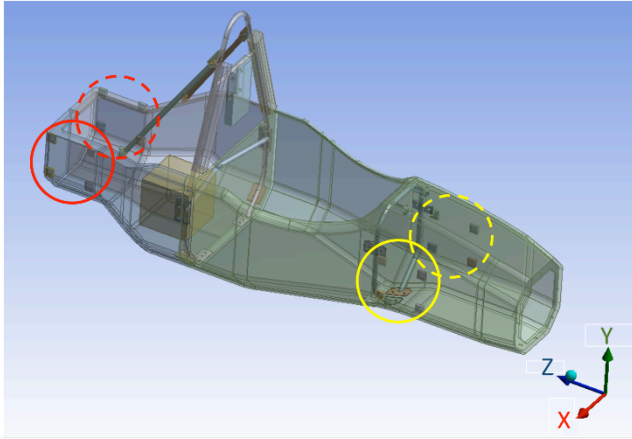

Fig. 1 Analytical model.

Table 1 Specifications of racing car.

Model	A	B
Overall length [mm]	3100	3075
Overall height [mm]	1243	1237
Overall width [mm]	1400	1440
Wheel base [mm]	1600	1700
Monocoque mass [kg]	51.5	50.6

performance. Therefore, the multiscale analysis is utilized to analyse the entire monocoque structure in FEM.

Figure 2 shows the honeycomb structure used in this analysis, then this is the unit cell and is regarded as the microscale model to practice the multiscale analysis. Here, the coordinates y_1, y_2 and y_3 are introduced anew in this figure, and the arbitrary displacements on sides A and B are denoted by u_1^A and u_1^B in y_1 direction and are defined as follows[8]:

$$u_1^A = \varepsilon_{11}y_1^A + \varepsilon_{12}y_2^A + \varepsilon_{13}y_3^A + u_1^{A*}, \tag{1}$$

$$u_1^B = \varepsilon_{11}y_1^B + \varepsilon_{12}y_2^B + \varepsilon_{13}y_3^B + u_1^{B*}. \tag{2}$$

The suffixes 1, 2 and 3 indicate y_1, y_2 and y_3 directions and the suffixes A and B mean the arbitrary positions on the sides A and B. ε_{ij} is a strain component in the tensor field and u_1^{A*} and u_1^{B*} are periodic disturbances caused by the structural heterogeneity.

According to the above indications of the arbitrary displacements on sides A and B, the displacements U_1^{AB}, U_2^{AB} and U_3^{AB} between the sides A and B can be expressed as follows:

$$\begin{Bmatrix} U_1^{AB} \\ U_2^{AB} \\ U_3^{AB} \end{Bmatrix} = \begin{Bmatrix} u_1^B \\ u_2^B \\ u_3^B \end{Bmatrix} - \begin{Bmatrix} u_1^A \\ u_2^A \\ u_3^A \end{Bmatrix} = \begin{bmatrix} \varepsilon_{11} & \varepsilon_{12} & \varepsilon_{13} \\ \varepsilon_{21} & \varepsilon_{22} & \varepsilon_{23} \\ \varepsilon_{31} & \varepsilon_{32} & \varepsilon_{33} \end{bmatrix} \left(\begin{Bmatrix} y_1^B \\ y_2^B \\ y_3^B \end{Bmatrix} - \begin{Bmatrix} y_1^A \\ y_2^A \\ y_3^A \end{Bmatrix} \right)$$

$$= \begin{bmatrix} \varepsilon_{11} & \varepsilon_{12} & \varepsilon_{13} \\ \varepsilon_{21} & \varepsilon_{22} & \varepsilon_{23} \\ \varepsilon_{31} & \varepsilon_{32} & \varepsilon_{33} \end{bmatrix} \begin{Bmatrix} l_1^{AB} \\ l_2^{AB} \\ l_3^{AB} \end{Bmatrix}, \tag{3}$$

where l_1^{AB}, l_2^{AB} and l_3^{AB} are the distances in the respective directions between the sides A and B, and then it is assumed to cancel out the periodic disturbances. Such a relationship functions not only between the sides A and B but also between other sides.

In actual numerical analysis, stress analysis is executed with the displacement constraint conditions based on Eq. (3). The stress is integrated in the unit cell and its volume average is obtained, so that elastic coefficients of the homogenized unit cell can be determined.
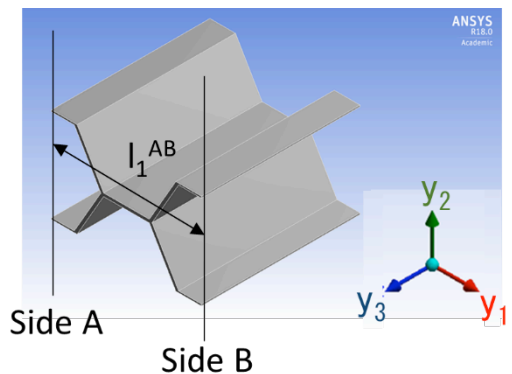

Fig. 2 Microscale model for honeycomb structure.

3. Results and Discussion

3.1 *Stress characteristics of monocoque structure*

The above honeycomb structure is made by aluminum alloy A5086, which has density of 2660 kg/mm³, Young's modulus of 70.6 MPa and Poisson's ratio of 0.33, and has foil thickness of 0.2 mm, length of a side of 3.0 mm, cell size of 5.2 mm and height of 10 mm. This honeycomb structure is regarded as the unit cell and FEM analysis with microscale model is carried out, so that the mechanical properties in the respective coordinate directions are obtained and are exhibited in Table 2.

Moreover, although these results are applied to the multiscale analysis using ANSYS to analyse the entire monocoque structure, both surfaces of the honeycomb structure are covered by CFRP plates whose thickness is 1 mm. This CFRP material is provided as the application of ANSYS, and its Young's modulus is 121 GPa in the direction of the carbon fiber and is 8.60 GPa in the normal direction of the fiber. The shear modulus and Poisson's ratio are 4.70 GPa and 0.27 in the plane including the carbon fiber axis and are 3.10 GPa and 0.40 in other planes.

In the whole analysis for the monocoque structure, the structure is subjected to the external force of 1000 N, which is loaded in the directions of *X*, *Y* and *Z*, (i.e. the forces in the directions of yaw, pitch and compression), respectively. On the other hand, the external force in the direction of the roll is expressed by -500 N and 500 N in *Y* direction and is applied clockwise with respect to the *Z* axis.

Figure 3 shows an example of the analysis results, in which Models A and B are subjected to the force in the yaw direction. The stress distributions are indicated in the *XZ* plane to estimate the strength characteristics, von Mises stress is used in these results. The area where the stress becomes larger is distributed widely due to monocoque characteristics. It is recognized that such an area of Model A extends to wider area than that of Model B. However, in Model B, it is also confirmed that such an area extends to the side walls of the cockpit and the plate partitioning off the cockpit and engine space.

3.2 *Factor to evaluate monocoque rigidity*

Figure 4 shows the deformation situation in the *XY* plane, when the monocoque structure is subjected to the forces in the roll direction. However, the deformation is enlarged to 640 times in comparison with the actual deformation by the function that ANSYS has, being too small and being hardly distinguished in the difference between the unloaded and loaded situations. In general, the estimation of such a deformation is practiced in the maximum value, whereas it is hard to examine accurately the structural rigidity of the monocoque with just that. Therefore, the centroid and sectional secondary moment are investigated in arbitrary cross-sectional planes (*XY* planes).

Here, the *x* and *y* coordinates are defined newly as shown in Fig. 5. The areas, and sectional primary and secondary moments in *xy* planes are calculated by using Gauss's theorem, which is established in a closed space[9]. The area *A* is obtained by setting x_i and y_i, which are the respective *x* and *y* coordinates in *n* divisions of the closed curve, as follows:

$$A = \frac{1}{2}\sum_{i=1}^{n}(x_i y_{i+1} - x_{i+1} y_i). \qquad (4)$$

Then the sectional primary moments S_x and S_y with respect to *x* and *y* axes are calculated from the following equations, Fig.

Table 2 Mechanical properties of unit cell.

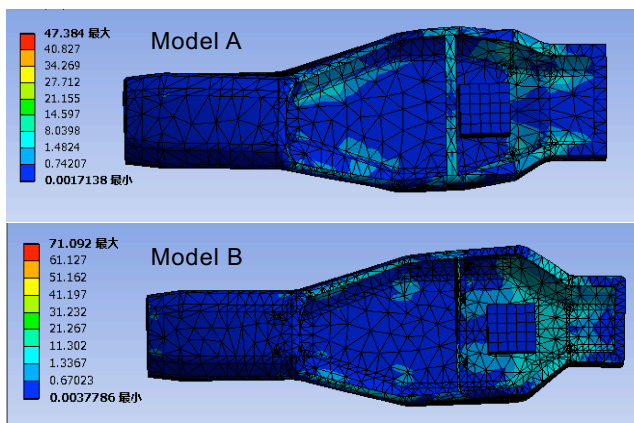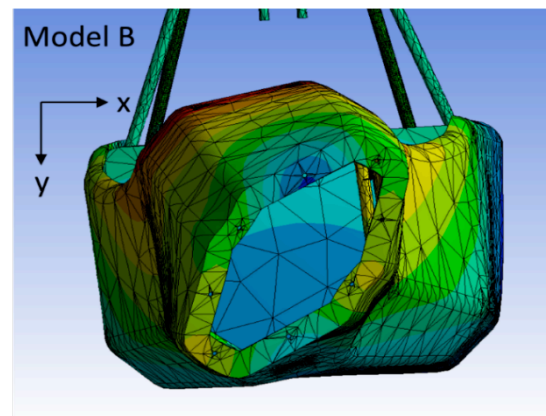| Coordinate	y_1	y_2	y_3
Young's modulus [MPa]	63.7 (E_{11})	75.7 (E_{22})	49.1×10^3 (E_{33})
Shear modulus [MPa]	23.9 (G_{12})	9.96×10^2 (G_{23})	9.16×10^2 (G_{13})
Poisson's ratio	0.892 (v_{12})	6.09×10^{-3} (v_{23})	3.32×10^{-3} (v_{13})

Fig. 3 Stress distribution of monocoque structure.

Fig. 4 Deformation state of twisted monocoque.

—9—

respectively.

$$S_x = \frac{1}{6} \sum_{i=1}^{n} (x_i y_{i+1} - x_{i+1} y_i)(x_i + x_{i+1}), \qquad (5)$$

$$S_y = \frac{1}{6} \sum_{i=1}^{n} (x_i y_{i+1} - x_{i+1} y_i)(y_i + y_{i+1}). \qquad (6)$$

The central coordinates G_x and G_y of the sectional plane are derived from A, S_x and S_y and are induced from Eq. (7).

$$G_x = \frac{S_y}{A}, \quad G_y = \frac{S_x}{A}. \qquad (7)$$

On the other hand, the sectional secondary moments I_x and I_y with respect to x and y axes are obtained from Eqs. (8) and (9), respectively.

$$I_x = \frac{1}{6} \sum_{i=1}^{n} (x_i y_{i+1} - x_{i+1} y_i)\{(y_i + y_{i+1})^2 + y_i^2 + y_{i+1}^2\}, \quad (8)$$

$$I_y = \frac{1}{6} \sum_{i=1}^{n} (x_i y_{i+1} - x_{i+1} y_i)\{(x_i + x_{i+1})^2 + x_i^2 + x_{i+1}^2\}. \quad (9)$$

These I_x and I_y are applied to the parallel axis theorem, so that the sectional secondary moments I_{Gx} and I_{Gy} with respect to the axes, which are parallel to x and y axes and pass through the centroid, are gotten, respectively. From these I_{Gx}

and I_{Gy}, new factor I_{xy} is defined as follows:

$$I_{xy} = I_{Gx} + I_{Gy}. \qquad (10)$$

I_u in an unloaded condition is denoted by I_0 and it is used in later examination.

The convergence of the above factor values should be evaluated with changes in n divisions, depending strongly on the division number. Figure 5 shows the cross-sectional area A as functions of n at $Z = 1110$ mm in Model B, which is not only unloaded but also is subjected to the twisting load. Then the position is where the cockpit width is extending with increasing Z (refer to Figs. 3 and 7). The area A increases greatly with n and varies widely until n reaches around 50 in both cases. The area A has a convergence tendency beyond such a n region and converges into the respective values. Actually, both convergence values should be so close, whereas the difference of them is clear because the deformation of the loaded model was enlarged to 640 times in comparison with the actual that.

The cross-sectional shapes and their centroids in the above cross sections are compared in the unloaded and loaded cases in Fig. 6. The shapes and centroids are exhibited in circles and crosses and the unloaded and loaded cases are distinguished in blue and red plots. Then the n is set to 600 divisions and the display magnification remains 640 times. The structural deflection and moving centroid can be grasped very well from this figure.
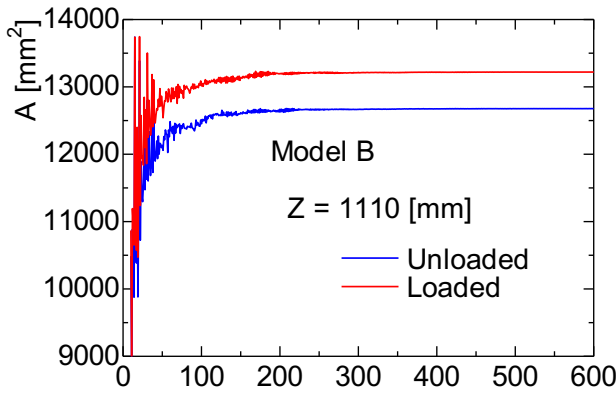

Fig. 5 Cross-sectional area as functions of division number.
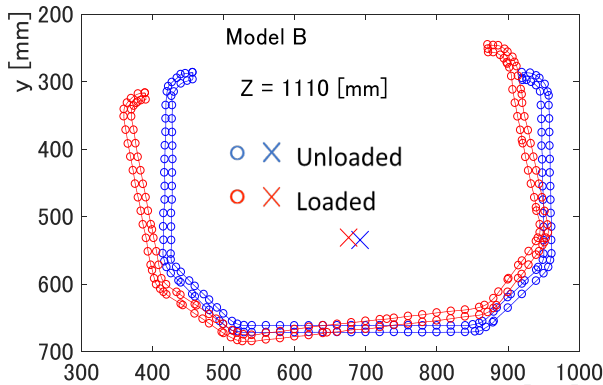

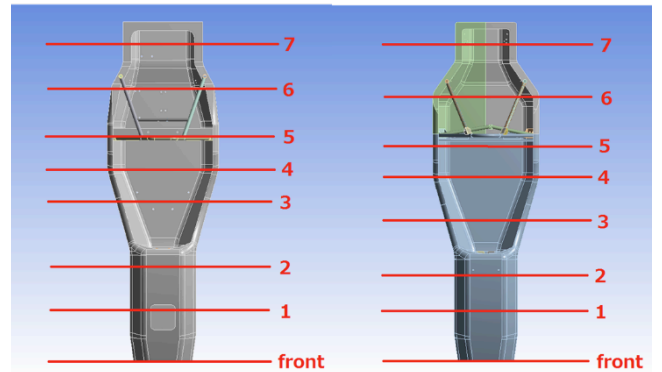Fig. 6 Deformation state and movement of centroid on cross-section.

Fig. 7 Cross section where movement of centroid and sectional secondary moment are examined.

Table 3 Z coordinate of examined cross section.

Position	Model A [mm]	Model B [mm]
1	336.4	383.9
2	597.8	614.5
3	1031	1110
4	1294	1308
5	1461	1537
6	1877	1901
7	2147	2263

3.3 *Rigidity characteristics of monocoque structure*

Here, in order to evaluate rigidity characteristics of the monocoque structure, the moving distance of the centroid and variation in sectional secondary moment attract attention as evaluation points with respect to an arbitrary *xy* plane. Such a plane is the cross-sections on the lines drawn in the respective models as shown in Fig. 7. The specific positions are exhibited in Table 3 and are described by *Z* coordinate from the front end, so that the *xy* plane in Figs. 5 and 6 corresponds to Position 3 in Model B.

The moving distance of the centroid is denoted by subtraction values ΔG_x and ΔG_y, which are calculated by subtracting the loaded G_x and G_y from the unloaded values, respectively. However, the loaded G_x and G_y are the actual centroid coordinates, not being enlarged as before. Figure 8 shows ΔG_y as functions of *Z* in Models A and B, when the forces in the directions of compression, pitch and yaw are applied to the monocoque structure and the twisting force in the direction of the roll is also applied to that. In both models, ΔG_y in the pitch direction decreases gradually with increasing *Z* from the maximum value at the front end and is minimized at Position 7. However, the other ΔG_y is uniformly maintained over the entire range of *Z* while having small variations.
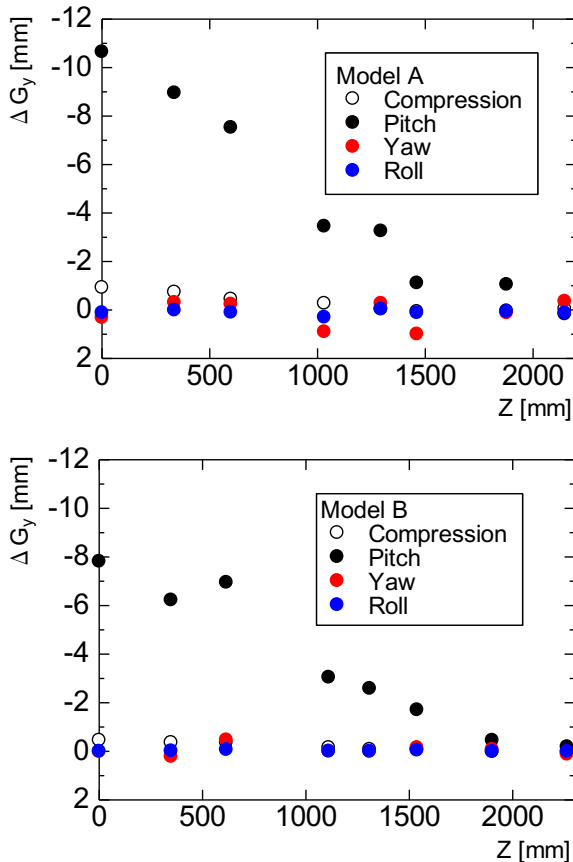
The great changes of ΔG_y in the pitch direction are caused by the correspondence between the moving and load directions and are maximized at the front end, near which the load is applied. Model B is suppressed more than Model A in not only those maximum ΔG_y but also the variation width of ΔG_y in the other loading conditions. On the other hand, the moving distance ΔG_x in the *x* direction is indicated in Fig. 9 and is plotted in the same manner as Fig. 8. ΔG_x increases in the load direction and is suppressed in the other directions, as with the consideration in Fig. 8.

Furthermore, in the larger ΔG_x and ΔG_y that occur in the correspondence between the moving and load directions, the decrease rate of ΔG_x is suppressed more than that of ΔG_y, in changing *Z*, and the tendency is remarkable in Model B. Then in the other directions, the variation width of ΔG_x is larger than that of ΔG_y and is promoted in Model A. These depend on symmetries with respect to *x* and *y* axes of the monocoque structure. Specifically, ΔG_y is the moving distance of the centroid on the *y* axis, about which the cross-section on *xy* plane is almost symmetric, whereas ΔG_x is on the axis of the asymmetric cross-section in the cockpit and the engine and differential gear spaces. Therefore, the variation width of ΔG_x becomes larger in the pitch and roll directions and is remark-
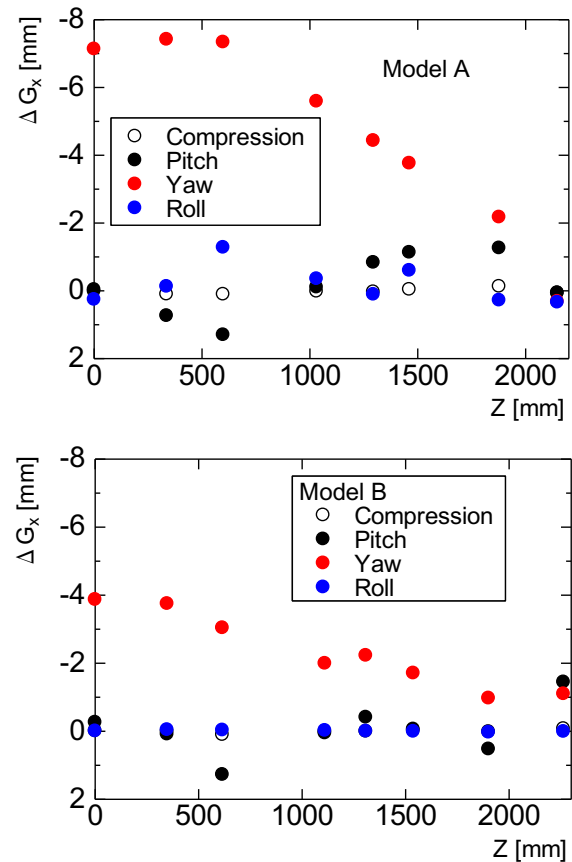

Fig. 8 Moving distance of centroid in *y* direction when monocoque is subjected to 4 kinds of loads, respectively.

Fig. 9 Moving distance of centroid in *x* direction when monocoque is subjected to 4 kinds of loads, respectively.

—11—

able particularly in Model A. Then the variation width of ΔG_y is also promoted relatively in the pitch and roll directions of Model A.

Taking into consideration the above estimation, it is supposed that Model B is intensified in the structural rigidity of the monocoque in comparison with Model A. However, Model B exceeds Model A in the variation width of ΔG_x at the differential gear space. This is because Model B is narrower than Model A in the width of the differential gear space (refer to Fig. 7).

The above estimation of the structural rigidity was carried out indirectly from the moving distance of the centroid. So, in order to attempt direct estimation of that, the sectional secondary moment is examined in the same cross-section. Although the structural rigidity should be evaluated by the respective sectional secondary moments I_{Gx} and I_{Gy} with respect to the x and y axes, the another sectional secondary moment I_{xy} is employed here. Summing I_{Gx} and I_{Gy} as described in Eq. (10), I_{xy} expresses overall bending characteristics with respect to the xy plane. Then, too, it also means approximately torsional characteristics with respect to the Z axis and the torsional rigidity is one of the most significant performances in actual racing cars.
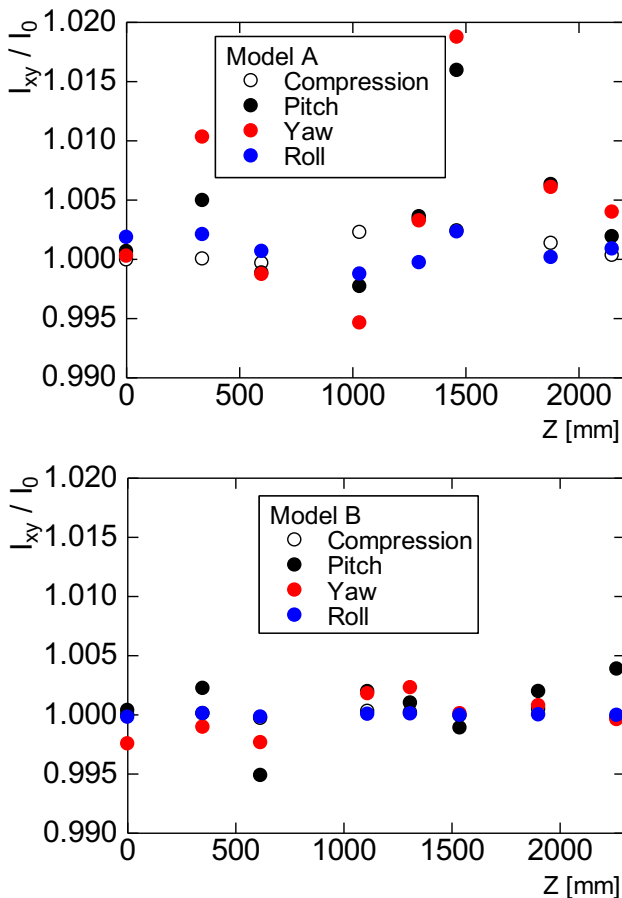
Being used as the factor for evaluating the structural rigidity, I_{xy} is divided by I_0, which corresponds with I_{xy} in the unloaded condition, and is made dimensionless. Figure 10 shows I_{xy} / I_0 as functions of Z in Models A and B, respectively, when each force is applied to the monocoque structure. I_{xy} / I_0 varies with Z and its variation width in Model A is much larger than that of Model B. In general, a structural rigidity depends greatly on the sectional secondary moment, so that the structural rigidity should be strengthened with increasing the sectional secondary moment. However, I_{xy} / I_0 herein is the factor to evaluate the degree of sectional deformation by applying the respective forces to the monocoque structure. The increase and decrease in I_{xy} / I_0 do not mean strengthening and weakening the rigidity but mean promoting the degree of sectional deformation. In other words, the approach to $I_{xy} / I_0 = 1.0$ shows weakening the degree and implies promoting the structural rigidity.

I_{xy} / I_0 of Model A increases in the yaw direction at $Z = 336.4$ and 1461 mm (Positions 1 and 5 in Fig. 7) and this is suggesting that those cross-sections have relatively large deformation. The increase in I_{xy} / I_0 at Position 2 is derived from the existence of the inspection hole that is crossed by the cross-section (refer to Model A in Fig. 7). Because the cross-section is not closed shape and becomes asymmetric with respect to the axis along the yaw direction, the structural rigidity is weakened relatively. Moreover, Position 5 is in the proximity of the boundary between the cockpit and engine space and has the widest opening, so that the rigidity lowering is remarkable. On the other hand, I_{xy} / I_0 is distributed in the vicinity of 1.0 with changing Z in Model B in comparison with that of Model A

According to the above results, i.e. the moving distance of the centroid and variation in the sectional secondary moment, it is obvious that Model B is superior to Model A in the structural rigidity. Actually, the racing cars, which the above monocoque structures were adopted, have taken part in Student Formula SAE Competition of Japan. The examination of this competition is classified roughly into tech inspection, static and dynamic events, and the dynamic events have some evaluation items that consist of acceleration, skidpad, autocross and endurance. Since the autocross is subjected strongly to the influence of the structural rigidity, the comparison between Models A and B is attempted in its results. Models A and B obtained 70.301 and 59.225 seconds as the respective records, which were the spent times for one round in the course of autocross.

Those actual results demonstrate that the evaluation of the structural rigidity is valid for the monocoque structure. In particular, a weak point of the monocoque structure could be found using variations in the sectional secondary moment. To

Fig. 10 Variation in sectional secondary moment when monocoque is subjected to 4 kinds of loads, respectively.

reflect such a result in a rational design of the monocoque structure, the design should be executed with evaluating the stress distribution characteristics. Then it is necessary to consider measures to make the monocoque structure more superior and it is a future significant matter for this study.

4. Conclusion

In this study, the monocoque structure for Student Formula, which was constructed of the honeycomb structure made by aluminum alloy and its surface plates made by CFRP, was adopted as the analytical model. The multiscale analysis was utilized to analyse the entire monocoque structure in FEM and the structural characteristics were investigated using the analysis results, as which the stress distribution and deformation were obtained. Particularly, with respect to its cross-section from the deformation, the moving distance of the centroid and variation in the sectional secondary moment attracted attention as significant evaluation factors. As a result, the following conclusion was obtained.

The area where the stress becomes larger is distributed widely and the monocoque characteristics, by which the internal force is dispersed in the whole structure, are captured. The moving distance of the centroid depends strongly on the load direction and increases greatly due to the correspondence with the load direction. Then the structural rigidity can be evaluated by the comparison of its moving distance. Moreover, the ratio between the sectional secondary moments based on loaded and unloaded situations is adopted to evaluate a degree promoting the sectional deformation, so the evaluation can accurately grasp the rigidity and also makes it

possible to determine weak points of the monocoque structure.

Acknowledgement

References

1) Website of Grandelfino (Kyoto Institute of Technology), http://www.grandelfino.net/.

2) Website of N.I.T. Formula Project (Nagoya Institute of Technology), http://www.qitc.nitech.ac.jp/formula/.

3) Website of SHIBAURA INSTITUTE OF TECHNOLO- GY FORMULA RACIMG (Shibaura Institute of Technology), http://shiba4.firebird.jp/TOP.html.

4) Website of TUT FORMULA (Toyohashi University of Technology), http://tut-f.com/.

5) Website of Tokai Formula Club (Tokai University), http://formula.shn.u-tokai.ac.jp/.

6) Website of Sophia Racing (Sophia University), https://www.sophiaracing.com/team.

7) Motion video of TUG Racing Team (Graz University of Technology), http://www.jsae.or.jp/formula/jp/.

8) N. Hirayama, Multiscale CAE using ANSYS – Numerical material examination using ANSYS, Website of ANSYS, http://www.cybernet.co.jp/ansys/product/lineup /multiscale/r elation/mono006.html.

9) Explanation of some properties with respect to cross-section, http://www.junko-k.com/cthema/43gauss.htm.